Resonant Raman studies of confined LO modes and interface modes in a small-period GaAs/AlAs superlattice

T. A. Gant,* M. Delaney, and M. V. Klein
Department of Physics, University of Illinois at Urbana-Champaign, 1110 West Green Street, Urbana, Illinois 61801

R. Houdré† and H. Morkoç
Coordinated Science Laboratory, University of Illinois at Urbana-Champaign, 1101 West Springfield Avenue, Urbana, Illinois 61801-3082

(Received 24 June 1988)

Resonant Raman scattering has been used to study the confined LO modes and interface modes near the lowest direct band gap of a GaAs/AlAs superlattice. We have studied the polarization dependence of the resonance profiles in detail. The peak positions of the polarized and depolarized resonance profiles are not the same. When the laser is polarized along (110) or (1$\bar{1}$0), we see an interference effect for some of these modes similar to that seen by Menéndez and Cardona in bulk GaAs. In bulk GaAs, this interference is an intrinsic effect. In superlattices, this effect is a violation of the selection rules for confined LO modes; we attribute this "forbidden" scattering by confined LO modes to an impurity-induced Fröhlich mechanism.

I. INTRODUCTION

Recently there has been much work on small-period GaAs/AlAs superlattices in which the lowest conduction band is derived from the X point of AlAs. Finkman and Sturge[1] were the first to identify these states on the basis of photoluminescence and excitation spectra. The transition from direct to indirect has been investigated experimentally[2] and theoretically.[3,4] From the point of view of resonant Raman scattering, these samples are an interesting system because one can do resonant Raman at the lowest direct band gap without having to worry about a large luminescence background obscuring the Raman signal.

Small-period superlattices exhibit interesting resonance Raman effects due to the complicated electronic structure and the well-separated confined LO modes. Phonons in superlattices which propagate normal to the layers are well understood.[5] The motivation in resonant Raman scattering is to study the electron-phonon interaction and the electronic structure. Resonance Raman studies of confined LO modes[6] and interface modes[7] have been reported by Sood *et al.* Meynadier *et al.*[8] reported the observation of higher-order Raman scattering by combinations and overtones of interface modes. In the present work we report a more detailed study of the polarization dependence of the resonance profile than has been reported before. For some of these modes, we see an interference effect in the $z(x'x')\bar{z}$ and $z(y'y')\bar{z}$ polarizations, similar to the work of Menéndez and Cardona[9,10] in bulk GaAs. This effect violates the usual selection rules for Raman scattering by confined LO modes in a superlattice.

II. EXPERIMENTAL DETAILS

The sample used for these measurements was a superlattice (21 Å GaAs)/(51 Å AlAs). The layer thicknesses were determined by x-ray diffraction. The optical measurements were performed at a temperature of 8 K. A pseudo-Brewster-angle backscattering geometry was used. Outside the sample, the laser beam makes an angle of approximately 70° with the normal to the surface. Inside the sample, this angle is reduced to 14° due to refraction. The wave vector $\mathbf{q}$ of the phonon is then 7° off of the [001] direction. This angle is small enough so that we can use the selection rules associated with exact backscattering. We have confirmed this by comparing spectra taken in the pseudo-Brewster angle and exact backscattering configurations. We have taken data in the $z(xx)\bar{z}$, $z(xy)\bar{z}$, $z(x'x')\bar{z}$, and $z(y'y')\bar{z}$ configurations,[11] where $x\|[100]$, $y\|[010]$, $z\|[001]$, $x'\|[110]$, and $y'\|[1\bar{1}0]$. The excitation source was a cw dye laser; both 4-(dicyanomethylene)-2-methyl-6-(*p*-dimethyl-amino-styryl)-4*H*-pyran (DCM) and Rhodamine-6G dyes were used. A Spex 1400 double monochromator was used to analyze the scattered light. The signal was detected by a photomultiplier tube in the photon counting mode. The resonance profiles are not corrected for absorption.

III. RESULTS AND DISCUSSION

A. PL and PLE

Figure 1 shows photoluminescence (PL) and photoluminescence excitation (PLE) spectra. The PL peak at 1.99 eV in Fig. 1 is at the lowest direct band gap. This is a weak luminescence peak; the luminescence at the indirect band gap (1.801 eV) is 2000 times stronger. The sharp structures on the high-energy side of the PL peak are higher-order Raman lines associated with the laser line exciting the luminescence. For the PLE spectrum, the monochromator was set at the peak of the indirect band-gap luminescence (1.801 eV) and the dye laser wavelength was stepped automatically, keeping the power constant. The PLE spectrum shows an absorption edge at

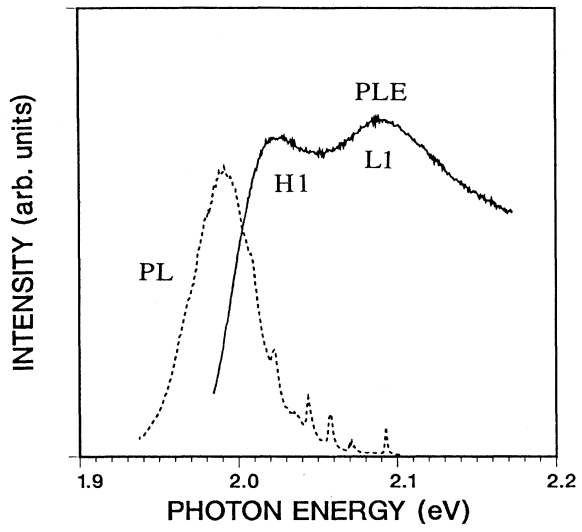

FIG. 1. Photoluminescence (dotted line) and PLE (solid line). For the PLE, the monochromator was set at the peak of the indirect band-gap luminescence at 1.801 eV. The sharp peaks in the high-energy tail of the PL are Raman lines associated with the exciting laser.

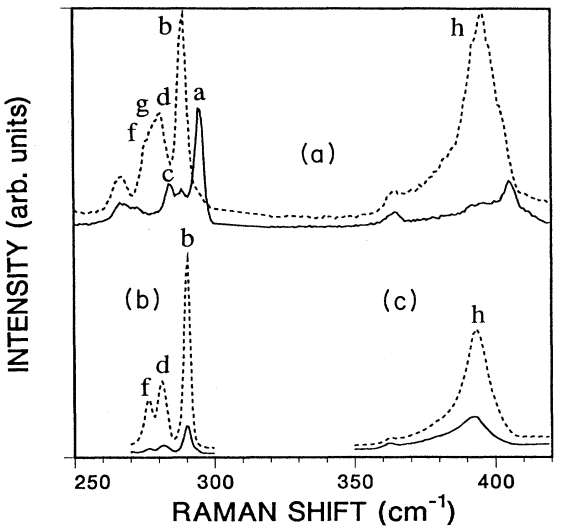

FIG. 2. Raman spectra at three different laser wavelengths: (a) laser, 2.41 eV; (b) laser, 2.039 eV; (c) laser, 2.074 eV. The spectra in (b) and (c) are near the peak of the resonance. For all three spectra: solid lines, $z(xy)\bar{z}$ polarization; dashed lines, $z(xx)\bar{z}$ polarization.

the position of the direct band-gap PL, and two peaks due to the $n=1$ heavy-hole (H) and light-hole (L) excitons at 2.02 and 2.09 eV, respectively. There is a shift between the PL peak and the H1 peak in the PLE spectrum. The PL occurs from the lowest energy state (an exciton bound to an impurity, or to monolayer fluctuations in well width), while the PLE peak is at the peak of the density of states (a band-to-band transition). Finkman *et al.*[1] also see such a shift. If we take a PLE spectrum with the monochromator set on the direct band-gap luminescence peak, the spectrum is dominated by Raman lines, as in Meynadier *et al.*[8]

B. Identifying the Raman peaks

Figure 2 shows Raman spectra taken at the peak of the resonance with the lowest direct band gap (bottom) and at 5145 Å (top). We see scattering from confined LO modes which we denote by LO_m. In the top curve [Fig. 2(a)], the confined LO modes (LO_1–LO_4 and LO_6) are seen in their allowed configurations: $z(xy)\bar{z}$ (depolarized) for the odd-order confined modes (B_2 symmetry) and $z(xx)\bar{z}$ (polarized) for the even-order confined modes (A_1 symmetry). In the bottom curve [Fig. 2(b)], the even-order confined LO modes (LO_2, LO_4, and LO_6) are observed in both the polarized and depolarized spectra. Interface optical phonons are also observed at 278 cm^{-1} in Fig. 2(a) (between the LO_4 and LO_6) and at 390 cm^{-1} in Figs. 2(a) and 2(c). The frequencies of the peaks in Fig. 2 are compared with calculated peak positions in Table I. The confined LO modes were calculated with the model of Levi *et al.*,[12] which takes into account the composition profile of the superlattice as determined by x-ray diffraction. This model assumes a parabolic dispersion for the LO mode of bulk GaAs, and thus overestimates the dispersion for the higher-order confined LO modes. This may provide the explanation for the large discrepancy (4 cm^{-1}) between the calculated and observed frequencies for LO_6. The interface optical-phonon frequencies were calculated using the $\mathbf{q}=0$ limit of the expression given in Sood *et al.*[7] These modes are wave vector forbidden, but are made Raman active by disorder (either impurities or interface roughness). The wave-vector allowed interface modes in backscattering are very close to the LO_1 and TO_1 frequencies, and cannot be resolved separately. Only the IF_1 and IF_4 interface modes are observed; these modes are of even parity and thus can be seen via an intraband-Fröhlich mechanism.[7] These interface modes are very similar to those observed by Sood *et al.*[6,7] in a sample similar to ours. If we take spectra at shorter wavelengths (i.e., the other Ar^+ lines) the LO_1 peak disappears and the 288-cm^{-1} peak broadens asymmetrically on the high-energy side. This probably represents scattering by interface modes when in resonance with electronic levels that are not confined.

The bottom curve in Fig. 2 shows four peaks—the 390-cm^{-1} interface mode (IF_4), and three peaks in the GaAs region at 290 cm^{-1} (LO_2), 281 cm^{-1} (LO_4), and 275 cm^{-1} (LO_6). This is a very strong resonance: the peaks in the bottom curve are roughly 10^4 times stronger than the same peaks in the top curve. All of these peaks are seen in both the polarized and depolarized spectra, in spite of the fact that the allowed scattering from even-order LO modes is polarized only, a phenomenon also observed by Sood.[6] This "forbidden" (xy) scattering is also seen in exact backscattering, and thus is not "leakage" due to the nonexact backscattering used here. Note the shift in the frequency of the LO_2 mode between Figs. 2(a)

TABLE I. Calculated frequencies for confined LO modes (LO_m) and $q=0$ interface modes (IF_1–IF_4) compared with the frequencies of the peaks in Fig. 2.

Mode	Label	ω calculated	2.41 eV (xx)	2.41 eV (xy)	2.039 eV	2.074 eV
LO_1	a	294.7		294.3		
LO_2	b	291.1	288.0		290.0	
LO_3	c	286.2		284.0		
LO_4	d	281.0	280.0		281.0	
LO_5		274.5				
LO_6	f	271.5	275.5		276.0	
IF_1	g	278.3	278.0			
IF_2		288.0				
IF_3		372.3				
IF_4	h	390.3	393.0			392.0

(288 cm^{-1}) and 2(b) (290 cm^{-1}). The resonant spectra [Fig. 2(b)] may be due to impurity-induced Fröhlich scattering, which would result in scattering by phonons with a high in-plane wave vector. The shift is due to the dispersion of this mode versus an in-plane wave vector. On the high-energy side of the resonance, the 275- and 281-cm^{-1} peaks gradually blur together due to the appearance of the IF_1 interface mode, resembling the structure in the top dashed curve.

C. Resonance profiles

Resonance profiles of these four peaks are plotted in Figs. 3 and 4, for both the polarized and depolarized scattering. We want to compare the peak positions with the energies of the H1 and L1 transitions indicated in Fig. 1 to see if any of these peaks can be attributed to in or out resonances with these transitions. First we examine the polarized resonance profiles. For the three GaAs modes the resonance profiles are very similar; there is a peak at 2.035 eV and a weak shoulder at 2.00 eV for all three curves. For the AlAs interface mode (Fig. 6), the peak is at 2.05 eV. All four of these peaks are shifted by their respective phonon energies from ≈ 2.00 eV, suggesting an out resonance. It is interesting to note that the resonance is not associated with the 2.02-eV peak in the PLE spectrum, which represents the peak of the density of states, but is closer to the 1.99-eV PL peak. Turning to the depolarized resonance profiles (Fig. 4), we see that the profiles for the LO_2, LO_4, and LO_6 modes are again similar; they all have a peak at 2.04 eV and a shoulder at 2.065 eV. The depolarized resonance profile for the IF_4

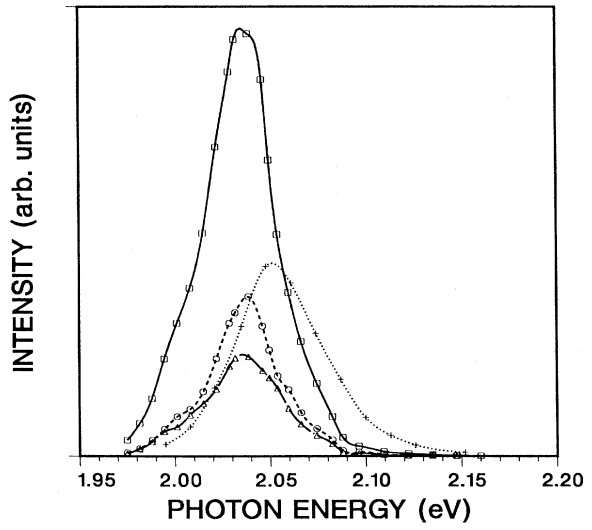

FIG. 3. Resonance profiles for the polarized $[z(xx)\bar{z}]$ scattering from the LO_2 mode (solid line), the LO_4 mode (dashed line), the LO_6 mode (chain-dotted line), and the IF_4 mode (dotted line). The symbols show the actual data points; the lines are a guide for the eye. Here and in Fig. 4 the LO_2, LO_4, and LO_6 have been plotted on the same scale; the IF_4 mode has been multiplied by a factor of 2.5 for clarity.

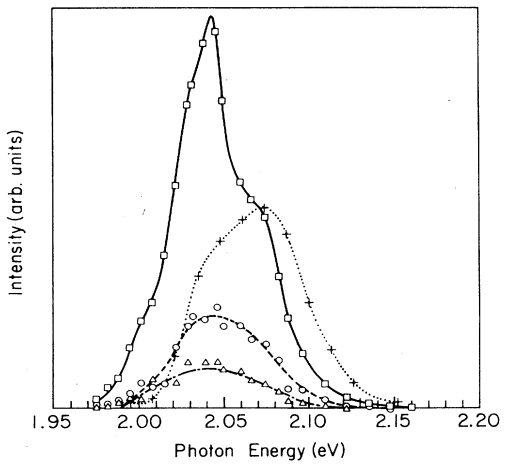

FIG. 4. Resonance profiles for the depolarized $[z(xy)\bar{z}]$ scattering, from the LO_2 mode (solid line), the LO_4 mode (dashed line), the LO_6 mode (chain-dotted line), and the IF_4 mode (dotted line). The symbols show the actual data points; the lines are a guide for the eye.

interface mode has a peak at 2.07 eV and a shoulder at 2.04 eV.

In resonance, the dominant part of the Raman cross section is proportional to[13]

$$\left| \sum_{\alpha,\beta} \frac{\langle 0|\mathbf{P}\cdot\hat{\epsilon}_S^*|\alpha\rangle\langle\alpha|H_{eL}|\beta\rangle\langle\beta|\mathbf{P}\cdot\hat{\epsilon}_L|0\rangle}{(E_S-E_\alpha)(E_L-E_\beta)} \right|^2 , \quad (1)$$

where $\hat{\epsilon}_L$ and $\hat{\epsilon}_S$ are the polarizations of the incident and scattered photons, H_{eL} is the electron-phonon interaction (Fröhlich plus deformation potential), E_S is the scattered photon energy, E_L is the incident photon energy, $|\alpha\rangle$ and $|\beta\rangle$ are intermediate states consisting of an electron-hole pair, and E_α and E_β are the energies of the intermediate states. The usual mechanism for resonance Raman scattering by LO phonons in bulk GaAs is intraband Fröhlich scattering. In that case, $\alpha=\beta$ and the expression above is symmetric in ω_S and ω_L. This would lead to in and out resonances of equal strength, something which is not the case here. Stronger out resonances have been observed before in quantum-well structures, and a variety of explanations have been put forth to explain this asymmetry. Zucker *et al.*[14] have explained asymmetric resonance profiles by including interband terms in Eq. (1), with intersubband-Fröhlich coupling. Sood *et al.*,[6] and more recently Kauschke *et al.*,[15] explain asymmetric resonance profiles as being due to impurity-induced intraband-Fröhlich coupling. Returning to Fig. 4, we notice that the depolarized resonance profiles tend to have two peaks, or one peak and a shoulder, which implies that the Raman tensor for these modes is dominated by interband terms. This is not the case for the polarized resonance profiles (Fig. 3), which display only one peak, consistent with intraband-Fröhlich coupling.

D. Interference effect

We have also looked at these resonance profiles in the $z(x'x')\bar{z}$ and $z(y'y')\bar{z}$ geometries. Menéndez *et al.*[9,10] have shown that in bulk GaAs the allowed and forbidden LO phonon scattering interfere when the laser is polarized along x' or y'. The allowed (deformation-potential) scattering is in the $z(xy)\bar{z}$ configuration; the forbidden (intraband Fröhlich) scattering is in the $z(xx)\bar{z}$ configuration. When the laser is polarized along x' or y', the allowed and forbidden scattering are both polarized. The two mechanisms will interfere. This interference exhibits itself as different scattering intensities for the $z(x'x')\bar{z}$ and $z(y'y')\bar{z}$ spectra. If the forbidden scattering from bulk GaAs is a combination of intrinsic and impurity-induced mechanisms, the intrinsic part of the forbidden scattering will interfere with the allowed scattering.[9]

In a superlattice the allowed scattering from A_1 symmetry confined LO phonons is polarized. In resonance, we see both polarized and depolarized scattering from these modes, as described above. This led us to look for this "interference" effect in a superlattice. In Fig. 5 we plot the resonance profiles of the LO_2, LO_4, and LO_6 modes for the $z(x'x')\bar{z}$ and $z(y'y')\bar{z}$ configurations. There is a weak interference for all three of these modes.

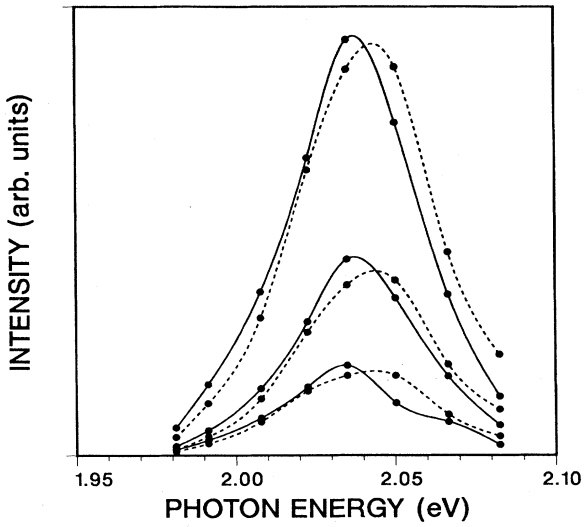

FIG. 5. Resonance profiles for the LO_2 mode (top), the LO_4 mode (center), and the LO_6 mode (bottom). Solid lines, $z(x'x')\bar{z}$; dashed lines, $z(y'y')\bar{z}$. The lines are a guide to the eye; the dots show the actual data points. The LO_2 and LO_6 have been plotted on the same scale; the LO_4 has been multiplied by a factor of 1.5 for clarity.

The interference acts to shift the peak position, rather than to change the intensity at the peak. This is quite different from the analogous effect in bulk GaAs.[9,10] In Fig. 6 we see that this interference effect is not present for the 390-cm^{-1} interface mode, as is expected for a disorder-activated mode.[9]

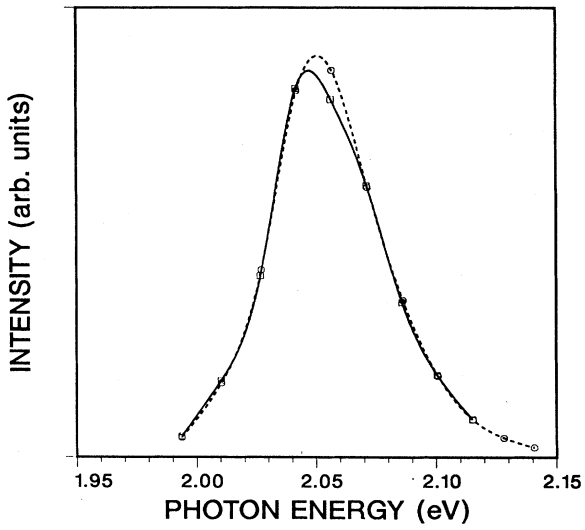

FIG. 6. Resonance profiles for the IF_4 mode in the $z(x'x')\bar{z}$ (solid line) and the $z(y'y')\bar{z}$ (dashed line) polarizations. The symbols show the actual data points; the lines are a guide to the eye.

IV. THEORY

The explanation of the interference effect is closely connected with the explanation of the forbidden depolarized scattering by A_1 symmetry modes. Since the depolarized scattering is forbidden, it is probably not an intrinsic process. We believe that it is due to impurity-induced Fröhlich scattering.[16] The allowed [i.e., $z(xx)\bar{z}$] scattering has both intrinsic and extrinsic contributions. We must show that the extrinsic part of the allowed scattering can interfere with the forbidden scattering.

Gogolin and Rashba[17] have shown how impurities can enhance the intraband-Fröhlich mechanism when in resonance in bulk semiconductors. In superlattices there is mixing between the heavy-hole and light-hole valence bands (for in-plane wave vectors)[18] which is not the case for bulk semiconductors. When we apply the Gogolin and Rashba mechanism to a superlattice, we must consider two-band terms. This is illustrated in Fig. 7. The contribution to the Raman cross section is proportional to

$$\sum_q \left| \frac{\langle 0|\mathbf{p}\cdot\hat{\epsilon}_S^*|\Psi_{\mathrm{H1},0}\rangle g(\mathbf{q})\langle\Psi_{\mathrm{H1},\mathbf{q}}|H_{\mathrm{imp}}|\Psi_{\mathrm{H1},0}\rangle\langle\Psi_{\mathrm{H1},0}|\mathbf{p}\cdot\hat{\epsilon}_L|0\rangle}{(E_S-E_{\mathrm{H1}})[E_L-E_{\mathrm{H1}}(\mathbf{q})+i\eta](E_L-E_{\mathrm{H1}})} + \frac{\langle 0|\mathbf{p}\cdot\hat{\epsilon}_S^*|\Psi_{\mathrm{H1},0}\rangle g(\mathbf{q})\langle\Psi_{\mathrm{H1},\mathbf{q}}|H_{\mathrm{imp}}|\Psi_{\mathrm{L1},0}\rangle\langle\Psi_{\mathrm{L1},0}|\mathbf{p}\cdot\hat{\epsilon}_L|0\rangle}{(E_S-E_{\mathrm{H1}})[E_L-E_{\mathrm{H1}}(\mathbf{q})+i\eta](E_L-E_{\mathrm{L1}})} \right|^2, \tag{2}$$

where $g(\mathbf{q})$ is the Fröhlich matrix element and H_{imp} is the Hamiltonian for exciton-impurity scattering. In a superlattice interface roughness may also play an important role; H_{imp} must include these effects as well. The subscripts H1 and L1 on E and Ψ refer to the energies and wave functions of the excitons derived from the H1 and L1 subbands. This is an important point; the Gogolin and Rashba mechanism depends on the intermediate states being excitons, and not uncorrelated electron-hole pairs. We have omitted the spin index; the bands H1 and L1 are each doubly degenerate; so there are actually four terms in Eq. (2). The first term in Eq. (2) is a one-band term and gives polarized scattering. The second term in Eq. (2) is a two-band term and gives depolarized scattering. This is most easily seen if we assume circularly polarized light. If $\hat{\epsilon}_L=1/\sqrt{2}(\hat{\mathbf{x}}+i\hat{\mathbf{y}})$ then the one-band term gives $\hat{\epsilon}_S=1/\sqrt{2}(\hat{\mathbf{x}}+i\hat{\mathbf{y}})$ and the two-band term gives $\hat{\epsilon}_S=1/\sqrt{2}(\hat{\mathbf{x}}-i\hat{\mathbf{y}})$. In reaching this result we are assuming that the impurity potential couples the initial light-hole state with the light-hole part of the "heavy-hole" state at finite q. The light-hole to heavy-hole transition is due to the valence-band mixing.

In evaluating Eq. (2) we follow the method used by Gogolin and Rashba. The sum over $\mathbf{q}$ is converted to an integral ($\mathbf{q}$ is in the xy plane). We assume an isotropic exciton dispersion (in the plane): $E_{\mathrm{H1}}(\mathbf{q})=E_{\mathrm{H1}}+\hbar^2q^2/2M$ where M is the mass of the heavy-hole exciton. The energy denominator $|1/[E_L-E_{\mathrm{H1}}(\mathbf{q})+i\eta]|^2$ becomes a Lorentzian divided by η, and this can be approximated by a δ function multiplied by (π/η). We are left with an integral over θ (the angle of $\mathbf{q}$ in the xy plane). The resulting expression is

$$\frac{A}{4}\frac{|g(q_0)|^2}{\pi\eta}\frac{M}{\hbar^2}\int_0^{2\pi}d\theta\left|F_{\mathrm{H1}}(\mathbf{q}_0)\frac{\langle 0|\mathbf{p}\cdot\hat{\epsilon}_S^*|\Psi_{\mathrm{H1},0}\rangle\langle\Psi_{\mathrm{H1},0}|\mathbf{p}\cdot\hat{\epsilon}_L|0\rangle}{(E_S-E_{\mathrm{H1}})(E_L-E_{\mathrm{H1}})}+F_{\mathrm{L1}}(\mathbf{q}_0)\frac{\langle 0|\mathbf{p}\cdot\hat{\epsilon}_S^*|\Psi_{\mathrm{H1},0}\rangle\langle\Psi_{\mathrm{L1},0}|\mathbf{p}\cdot\hat{\epsilon}_L|0\rangle}{(E_S-E_{\mathrm{H1}})(E_L-E_{\mathrm{L1}})}\right|^2, \tag{3}$$

where $F_{\mathrm{H1}}(\mathbf{q})$ and $F_{\mathrm{L1}}(\mathbf{q})$ represent the matrix elements of H_{imp} in Eq. (2), A is the area of the sample in the xy plane, and $q_0\equiv[2M(E_L-E_{\mathrm{H1}})]^{1/2}/\hbar$. We are approximating the sum over q by taking only the most resonant contribution, $q=q_0$. In Eq. (3), there are actually four terms inside the absolute value signs because the H1 and L1 bands are doubly degenerate. The first term represents two terms with $\mathrm{H1}(\pm\frac{3}{2})\rightarrow\mathrm{H1}(\pm\frac{3}{2})$. The second term represents terms with $\mathrm{L1}(\pm\frac{1}{2})\rightarrow\mathrm{H1}(\mp\frac{3}{2})$. If the matrix element F_{L1} depends on band mixing, as we discussed, then it will depend on θ. We expect that F_{H1} does not depend on θ, but only on q. Zhu and Huang[18] give the angular dependence of the mixing between the subbands. The admixture of a $+\frac{1}{2}$ light-hole subband into a $-\frac{3}{2}$ heavy-hole subband is proportional to $e^{-2i\theta}$; the admixture of a $-\frac{1}{2}$ light-hole subband into a $+\frac{3}{2}$ heavy-hole subband is proportional to $e^{2i\theta}$. The angular dependence of the impurity matrix elements is then given by $F_{\mathrm{H1}}(\mathbf{q}_0)=F_{\mathrm{H1}}(q_0)$ and $F_{\mathrm{L1}}(\mathbf{q}_0)=F_{\mathrm{L1}}(q_0)e^{\pm 2i\theta}$, where the sign of the exponent depends on the spin state of the hole.

By summing over the intermediate states and evaluating the momentum matrix elements, Eq. (3) can be reduced to the expression

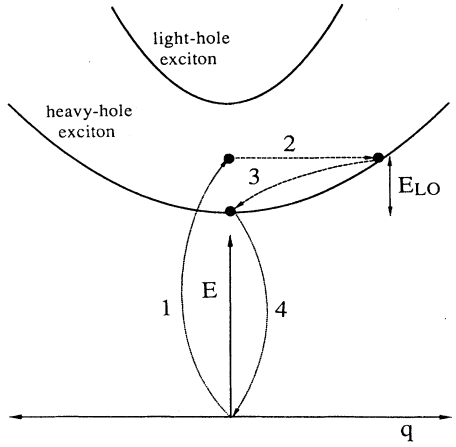

FIG. 7. An illustration of the impurity-induced intraband Fröhlich mechanism in a superlattice: (1) an incident photon is absorbed, creating an exciton which is an admixture of the heavy-hole and light-hole excitons; (2) this exciton scatters off of an impurity to a heavy-hole state at some in-plane wave vector q; (3) the exciton emits an LO phonon via the Fröhlich interaction and scatters back to $q=0$ in the same band; (4) the exciton recombines, emitting a scattered photon. The curves represent the dispersion of the heavy-hole and light-hole excitons vs an in-plane wave vector q.

$$\frac{A}{4}\frac{|g(q_0)|^2}{\pi\eta}\frac{M}{\hbar^2}\int_0^{2\pi}d\theta|\hat{\epsilon}_S^*\cdot\mathbf{R}(\theta)\cdot\hat{\epsilon}_L|^2\ , \tag{4}$$

where $\mathbf{R}(\theta)$ is a θ dependent Raman tensor which is given by

$$\mathbf{R}(\theta)=\begin{bmatrix} a-b\cos\theta & 2\sqrt{3}b\sin\theta & 0 \\ 2\sqrt{3}b\sin\theta & a+b\cos\theta & 0 \\ 0 & 0 & 0 \end{bmatrix} \tag{5}$$

and a and b are given by

$$a=\frac{|\bar{p}|^2F_{\mathrm{H1}}(q_0)}{(E_S-E_{\mathrm{H1}})(E_L-E_{\mathrm{H1}})}\ ,$$
$$b=\frac{\frac{1}{6}|\bar{p}|^2F_{\mathrm{L1}}(q_0)}{(E_S-E_{\mathrm{H1}})(E_L-E_{\mathrm{L1}})}\ . \tag{6}$$

In Eq. (4.7), $\bar{p}=\langle S|p_x|X\rangle$. S and X are the basis states in the Kane model.[19] If we transform $\mathbf{R}$ to the basis (x',y',z) we get

$$\mathbf{R}(\theta)=\begin{bmatrix} a+2\sqrt{3}b\sin\theta & -b\cos\theta & 0 \\ -b\cos\theta & a-2\sqrt{3}b\sin\theta & 0 \\ 0 & 0 & 0 \end{bmatrix}\ . \tag{7}$$

If we average $|\hat{\epsilon}_S^*\cdot\mathbf{R}(\theta)\cdot\hat{\epsilon}_L|^2$ over θ, we get for $z(xx)\bar{z}$ or $z(yy)\bar{z}$, $a^2+b^2/2$; for $z(xy)\bar{z}$ or $z(yx)\bar{z}$, $6b^2$; and for $z(x'x')\bar{z}$ or $z(y'y')\bar{z}$, a^2+6b^2. We do not get different intensities for the $z(x'x')\bar{z}$ and $z(y'y')\bar{z}$ as were observed.

The theory we have just outlined explains the depolarized scattering, but not the interference. This is probably due to the simplifying assumptions we made: the isotropic exciton dispersion and the angular dependence of the matrix elements $F(\mathbf{q})$. The actual form of the impurity potential is not known, but defects such as dislocations and interface roughness will have a much more complicated angular dependence for the impurity potential, and will probably lead to an interference.

V. CONCLUSION

We have studied the resonance profiles of the A_1 symmetry confined LO modes and an interface mode near the lowest direct band gap in four different configurations: $z(xx)\bar{z}$, $z(xy)\bar{z}$, $z(x'x')\bar{z}$, and $z(y'y')\bar{z}$. In the $z(xx)\bar{z}$ configuration all four phonons exhibit an out resonance with the H1 exciton. In the $z(xy)\bar{z}$ configuration the resonance profiles have a two peaked structure with peaks at the out resonance with H1 and the in resonance with L1. This implies interband transitions between the L1 and H1 subbands (more precisely, the excitons derived from these subbands). The three A_1 symmetry confined LO modes show an interference in the $z(x'x')\bar{z}$ and $z(y'y')\bar{z}$ spectra. Calculations of this effect are difficult because we don't know the explicit form of the impurity potential. We have given a mechanism which accounts for the forbidden $z(xy)\bar{z}$ scattering by A_1 symmetry confined LO phonons. With some simplifying assumptions, this mechanism did not give an interference. We believe that a more realistic form for the impurity potential will give an interference.

ACKNOWLEDGMENTS

This work was supported by the National Science Foundation (NSF) under Grant No. NSF-DMR-85-06674. The molecular-beam-epitaxy growth of the sample was funded by U.S. Air Force Office of Scientific Research (AFOSR). The x-ray diffraction measurements were performed in the University of Illinois Center for Microanalysis with the aid of J. McMillan. We would like to thank Y. C. Chang for useful discussions and M. Cardona for suggesting that the impurity-induced Fröhlich mechanism may be important.

*Present address: Division of Physics, National Research Council of Canada, Ottawa, Canada K1A 0R6.

†Present address: Laboratoire de Physique de la Matière Condensée, Ecolé Polytechnique, 91128 Palaiseau CEDEX, France.

[1]E. Finkman and M. D. Sturge, Appl. Phys. Lett. **49**, 1299 (1986).

[2]G. Danan, B. Etienne, F. Mollot, R. Planel, A. M. Jean-Louis, F. Alexandre, B. Jusserand, G. Le Roux, J. Y. Marzin, H. Savary, and B. Sermage, Phys. Rev. B **35**, 6207 (1987).

[3]J. Ihm, Appl. Phys. Lett. **50**, 1068 (1987).
[4]D. Z.-Y. Ting and Y. C. Chang, Phys. Rev. B **36**, 4359 (1987).
[5]M. V. Klein, IEEE J. Quantum Electron. **QE-22**, 1760 (1986).
[6]A. K. Sood, J. Menéndez, M. Cardona, and K. Ploog, Phys. Rev. Lett. **54**, 2111 (1985).
[7]A. K. Sood, J. Menéndez, M. Cardona, and K. Ploog, Phys. Rev. Lett. **54**, 2115 (1985).
[8]M. H. Meynadier, E. Finkman, M. D. Sturge, J. M. Worlock, and M. C. Tamargo, Phys. Rev. B **35**, 2517 (1987).
[9]J. Menéndez and M. Cardona, Phys. Rev. B **31**, 3696 (1985).
[10]J. Menéndez and M. Cardona, Phys. Rev. Lett. **51**, 1297 (1983).
[11]In the notation $i(jk)l$, i and l refer to the wave vectors of the incident and scattered photons, and j and k refer to their polarizations.
[12]D. Levi, Shu-Lin Zhang, M. V. Klein, J. Klem, and H. Morkoç, Phys. Rev. B **36**, 8031 (1987).
[13]M. Cardona, in *Light Scattering in Solids II*, edited by M. Cardona and G. Güntherodt (Springer-Verlag, Berlin, 1982), p. 19.
[14]J. E. Zucker, A. Pinczuk, D. S. Chemla, A. C. Gossard, and W. Wiegmann, Phys. Rev. Lett. **51**, 1293 (1983).
[15]W. Kauschke, A. K. Sood, M. Cardona, and K. Ploog, Phys. Rev. B **36**, 1617 (1987).
[16]A. Alexandrou, M. Cardona, and K. Ploog, Phys. Rev. B **38**, 2196 (1988).
[17]A. A. Gogolin and E. I. Rashba, Solid State Commun. **19**, 1177 (1976).
[18]B. Zhu and K. Huang, Phys. Rev. B **36**, 8102 (1987).
[19]E. O. Kane, J. Phys. Chem. Solids **1**, 249 (1957).